EVALUATION OF INTERNAL THERMAL GRADIENTS FROM SURFACE THERMOGRAPHY MEASUREMENTS: APPLICATION TO PROCESS CONTROL

A. Bendada, N. Nardini, and C. De-Granpré
National Research Council, Industrial Materials Institute, Boucherville, Quebec, Canada

Abstract: Infrared thermography is a real-time temperature mapping technique that allows to monitor surface thermal phenomena as functions of time. These surface phenomena are usually the result of heat transfer within the material under investigation. Comparison with a perfect heat transfer model then can yield relevant thermal information about the interior of the material. In this study, we show how surface infrared data can be used to recover the sub-surface temperature distribution via inverse heat conduction techniques. The developed algorithms have been applied to two typical industrial process examples. Firstly, to reconstruct the temperature profile over the thickness of a polymer preform during the injection-stretch-blowing process. Secondly, to predict thermal gradients along the radius of a cylindrical billet during induction heating of semi-solid light alloys. Both algorithms were validated using surface temperature data generated numerically. Then, they were applied to real data obtained using an infrared camera. Good correlation was found between the calculated temperature profiles and those obtained with thermocouples inserted within the material.

Introduction: In polymer processes such as extrusion, injection molding or blow molding, the material undergoes a complex history in which it is melted, flows through complex geometries where viscous dissipation plays a central role, is deformed to take the shape of the mold, and finally is cooled down and solidified into the final product. Therefore, temperature is one of the most important parameter in polymer processing since it has a large influence on the final properties of the product. However, its measurement is extremely difficult, especially its profile in the thickness direction. One of the difficulties is the nature of polymer processes in which the material solidifies to form the product so that invasive techniques such as thermocouple insertion are not applicable. Another difficulty is the lack of information on the initial temperature distribution which prevents the forward solution of the heat transfer equation. In this work, an inverse technique is developed to predict the initial temperature distribution in the thickness direction of a polyester (PET) preform from the surface temperature measurement.

The same procedure after minor modifications has been applied to the heating phase in the SSM forming process. Rather than using fully liquid alloys as in the conventional die-casting, the SSM forming process uses alloys that are typically 40% liquid and 60% solid. The commonly used technology for achieving this semi-solid state in commercial production applications is electromagnetic induction heating. The alloy is cut into cylindrical billets which are placed on vertical individual pedestals and subsequently introduced into cylindrical coils to be inductively heated. Each billet is then injected into a die and held there until solidified. At such a liquid fraction, the rheological properties of the semi-solid alloy are very sensitive to variations in the liquid phase portion [1]. Thus, it is extremely important to maintain the required liquid fraction constant and also ensure its uniform distribution throughout the heated billets prior to their injection into the die. The heating procedure must then be accurately controlled to allow a uniform temperature in the billets and the optimum semi-solid temperature for casting. But induction units have the drawback of non-uniform heating in the radial direction because of the “skin effect” and near the ends of the billet because of the “electromagnetic end effects” [2-4]. The “skin effect” is due to the fact that the generation of heat is concentrated at the surface and its density decreases nearly exponentially with distance from the outer surface to the core [2]. The “electromagnetic end effects” are essentially due to the distortion of the electromagnetic field at the ends of the workpiece and to additional radiation and convection heat losses in those areas as compared to the middle region [2-4]. Accurate control of the temperature in the whole billet at all stages of the heating process is thus a key element in successful SSM forming. The use of thermocouples, or any other invasive technique, is not very practical due to the nature of the SSM process itself. To bypass the invasive aspect of thermocouples, we used as for the ISBM process the infrared camera to monitor the surface temperature. These surface infrared data evolution with time are then used to predict the temperature distribution within the entire billet.

Results: In the first part of this section, we describe the investigation related to the ISBM process. In this process, a preform is injection molded, stretched by a rod to its final length and then inflated. The temperature distribution in

the preform has an important influence on the thickness uniformity of the final product and whether the preform can be stretched and inflated properly. In the following section, the temperature distribution in the thickness of the part is defined and solved as an inverse problem. The thickness of the part is usually much smaller than the other two dimensions. Therefore, it is reasonable to assume that the heat transfer is one-dimensional. Furthermore, since the temperature of the mold or die is controlled at approximately the same temperature on both sides, the temperature profile is considered symmetric across the mid plane of the thickness. With the above assumptions, the equations governing the temperature evolution in the preform are given by:

$$\rho C_p \frac{\partial T}{\partial t} = \frac{\partial}{\partial x} k \frac{\partial T}{\partial x} \tag{1}$$

$$k \frac{\partial T}{\partial x} = 0 \quad \text{at } x = 0 \text{ (on the plane of symmetry)} \tag{2}$$

$$-k \frac{\partial T}{\partial x} = h(T - T_a) \quad \text{at } x = d \quad \text{(on the surface)} \tag{3}$$

$$T(x, t = 0) = f(x) \tag{4}$$

where T is the temperature, T_a the ambient temperature, ρ the density, C_p the specific heat, k the thermal conductivity, h the heat transfer coefficient, t and x denote time and spatial coordinate, respectively and d is the half thickness of the part. The initial condition is simulated by the function f(x). If the initial temperature distribution over the thickness of the part is known, the problem is well-posed and a unique solution can be obtained. However, this temperature distribution is usually unknown and difficult to measure. On the other hand, the surface temperature of the part is measurable and is a direct consequence of the internal temperature distribution. The physical definition of this inverse problem is to reconstruct the unknown initial temperature distribution by measuring the surface temperature as a function of time after part ejection. By using different portion of the time response data, the heat transfer coefficient can also be identified.

Several techniques have been used for the solution of inverse problems including the regularized least square method [5, 6] the sequential estimation [5], the mollification method [7] and the conjugate gradient method using an adjoint equation [8, 9] in conjunction with the finite element method [10] or the boundary element method [11]. If the initial condition is varied by an amount $\Delta f(x)$, the surface temperature will vary by $\Theta(x,t)$. The function f(x) can thus be found by minimizing the functional J[f(x)] defined by:

$$J = \int_0^t [T_s(t) - T_m(t)]^2 dt \tag{5}$$

where T_s and T_m are, respectively, the computed and the measured surface temperature. In this work, the conjugate gradient iterative regularization method is applied to search for the minimum of the functional with the resulting equations solved by the finite element technique. This method has been well documented elsewhere [12-15] and will not be repeated here. In order for the algorithm to be efficient, several issues have to be considered. One of them is the number of nodes used to approximate the temperature profile. Another is the amount of data available. Insufficient data lead to error in the solution while too much data give rise to correlation between parameters. This is dealt with using a sensitivity analysis [14]. The analysis revealed that sensitivity coefficients S_{fm} to the initial temperature profile decreases with increasing the number of nodes. On the other hand, the analysis has showed that the measured surface temperature data used in the estimation of the initial temperature profile should be taken only over a short dimensionless time segment (Fourier number), $0 < t < t_0$, where t_0 is 0.3. At longer times, sensitivity coefficients S_{fm} are correlated. On the other hand, identification of the heat transfer coefficient is easier at longer times $t > t_0$ where the surface temperature is more sensitive to heat losses.

	Polyethylene Therephtalate (PET)	A356 aluminum alloy
Density (Kg/m^3)	1300	- 0.208 T + 2680

Specific Heat (J/Kg/°C)	1500 + 4 (T-105)	0.454 T + 904.6
Thermal Conductivity (W/m/°C)	0.245	0.04 T + 153.1
Heat Transfer Coefficient ($W/m^2/°C$)	15	5

Table 1. Thermophysical properties used in calculation.

The inverse algorithm is tested using the initial temperature profile shown in Figure 1b. The forward problem was first solved to generate the surface temperature using the parameters shown in Table 1. All thermal properties are assumed to be constant. This surface temperature was then used as "experimental" data to reconstruct the initial temperature profile using the inverse method. To assess the effect of noisy data on the reconstructed temperature profile, a 2% random noise with zero mean was superposed on the exact data. The exact data and those with noise are shown in Figure 1a. Figure 1b shows a comparison between the input and recovered temperature profiles.

Experimental validation trials were carried out in a single stage AOKI injection-stretch-blow-molding machine. An AGEMA 900 LW 8-12μm infrared camera was used to record the surface temperature of the preform as it was taken out of the injection mold and held in place at the thread region. The thickness of the preform is about 3mm. To ensure that the measured temperature is the surface temperature, a narrow wavelength filter centered at 8.93 μm was fitted to the camera. During the molding of the preform, a hot polymer melt at 270°C is injected into the cold cavity at about 20°C. While inside the cavity, the packing pressure keeps the polymer in contact with the mold resulting in a cold surface and a hot interior. When the preform is removed from the mold, which corresponds to time t = 0 s in the experiments, heat from the hot interior moves to the surface causing the temperature to rise. An infrared picture of the preform and a typical surface temperature-time plot are shown in Figures2 and 3a.

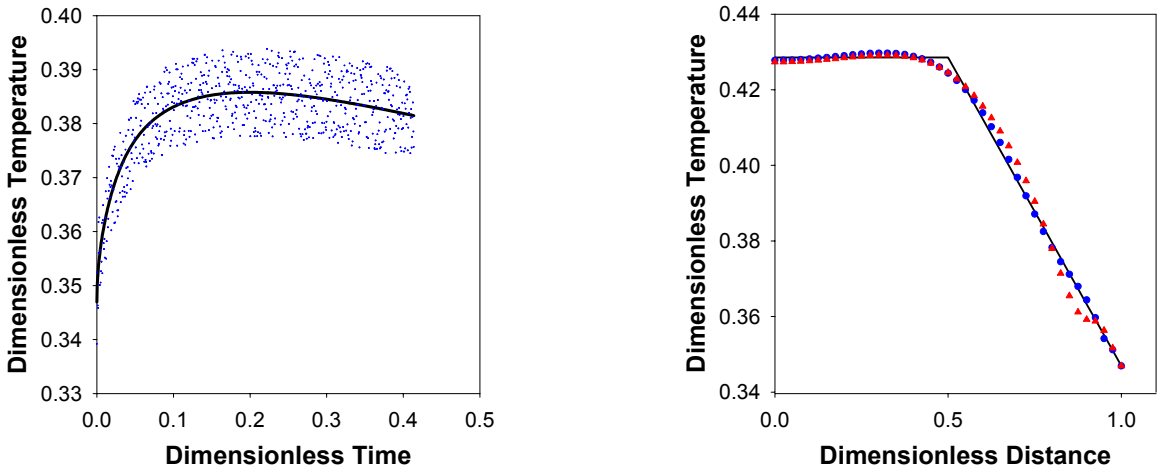

Figure 1. a. Surface temperature data generated numerically (exact (-), and noisy (+)) from an initial ramp function profile shown in Figure 1b. **b.** Comparison between the input initial temperature profile (-) and the reconstructed profiles when the data are exact (() and when the data contain 2% random noise (▲).

The inverse algorithm is now applied to the surface temperature data obtained from the infrared camera. Figure 3b shows the predicted temperature profile across the thickness of the preform from the centerline to the surface. The heat transfer coefficient h was estimated by a trial and error method. Using the measured surface temperature over a short dimensionless time segment $0 < t < 0.3$, the initial temperature profile is predicted. This profile is then used to calculate the "extrapolated" surface temperature, i.e., the surface temperature for longer dimensionless times $t > 0.3$. This "extrapolated" surface temperature tends to deviate from the measured temperature if an incorrect

value of heat transfer coefficient was used. The heat transfer coefficient h is adjusted and a new "extrapolated" surface temperature is calculated until it matches with the measured temperature.

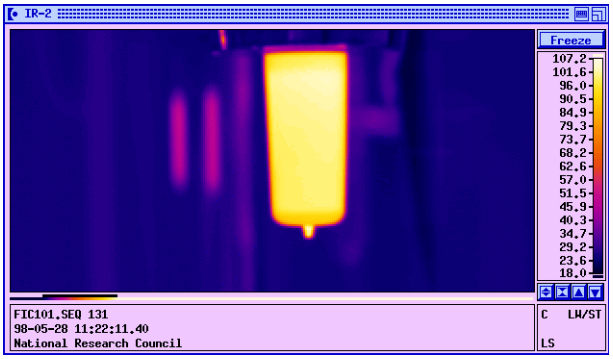

Figure 2. Shape and infrared image of the preform as it was taken out of the injection mold and held in place at the thread region.

In the second part of the current section, we describe the investigation related to the induction-heating phase during the SSM forming process. In this process, a metallic billet is first heated in an induction furnace until it reaches a semi-solid state. Then, it is injected into a die and kept there until it solidifies. The temperature distribution within the billet at the end of the heating phase is again of prime importance for the success of the process and the quality of the final product. The temperature distribution during heating is quite complicated. The concentration of heat near the billet surface caused by the "skin effect" is conducted toward the center and at the same time lost to the environment through convection and/or radiation. Figure 4 is an infrared image that illustrates the surface-to-core thermal gradients caused by the "skin effect" on the top surface of the billet during a typical induction heating cycle. In the following section, the temperature distribution along the radius of the billet before the alloy starts to melt (one-phase model to two-phase model is the subject of on-going research) is estimated using an inverse method. It is assumed that the heating is axisymmetric and uniform along the length of the billet, which is generally confirmed by a proper choice of design parameters. Indeed, it is possible to obtain a situation where the additional heat losses at the ends of the billet are compensated for by the additional energy (overheating) due to the "electromagnetic end effects". This will allow achieving a reasonably uniform temperature profile along the height of the billet. It is assumed further that the heat transfer by radiation is negligible. Then, the equations governing the temperature evolution in the billet at the end of the heating are given by:

$$\rho C_p \frac{\partial T}{\partial t} = \frac{1}{r}\frac{\partial}{\partial r} kr \frac{\partial T}{\partial r} \qquad (6)$$

$$k\frac{\partial T}{\partial r} = 0 \qquad (\text{at } r = 0) \qquad (7)$$

$$k\frac{\partial T}{\partial r} = h(T - T_a) \qquad (\text{on the surface}) \qquad (8)$$

$$T(r, t = 0) = f(r) \qquad (9)$$

where t and r denote time and spatial coordinate, respectively, R is the radius of the billet and f(r) is the initial temperature distribution. The inverse problem of reconstructing the initial condition of the billet in the radial direction is formulated as for the ISBM process using the conjugate gradient algorithm to minimize the functional J(f(r)) (Equation 5).

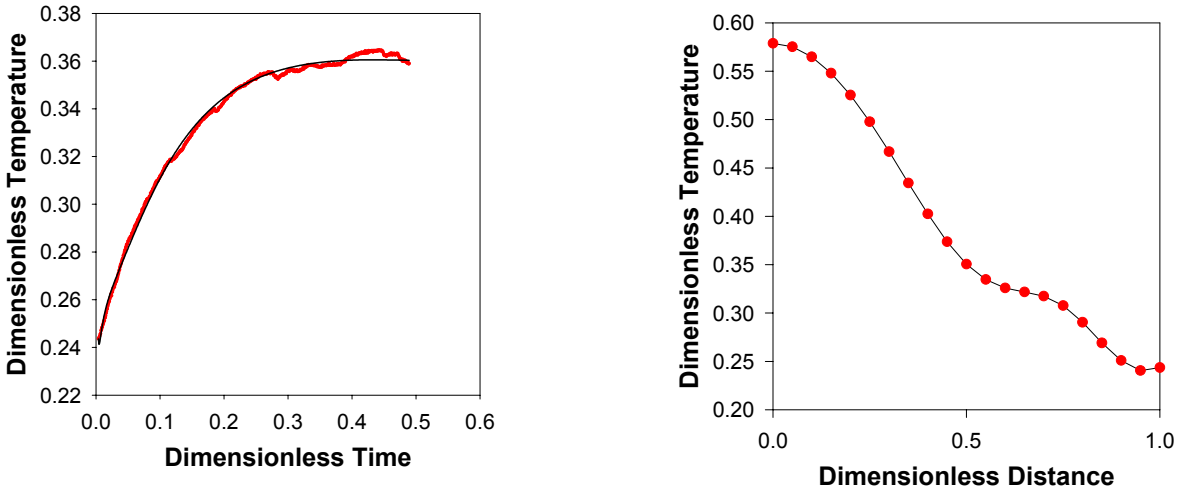

Figure 3. a. A typical plot of the measured temperature vs. time at one point on the surface of the preform and comparison with the predicted temperature. **b.** The initial temperature over the thickness of the preform just after it was taken out of the injection mold as reconstructed from the surface temperature data shown in Fig. 3a.

In order to test the algorithm, a possible temperature profile developed for a sample that is heated by induction and cooled down at the surface by convection is considered. The temperature profile is characterized by a peak between the centerline and the wall due to the competition between the heat conduction toward the center, the heat loss at the surface and the heat generation near the surface by the "skin effect". The position and the size of the peak depend on the relative importance of the individual factors in the particular experiment. This profile is estimated by a triangular temperature shape followed by a constant as depicted in Figure 5a. In the following calculations, a radius of 38 mm is used since this corresponds to the radius of the billets in the experiments. The forward problem was solved to generate exact and a 2% noisy surface temperature using the parameters shown in Table 1. Figure 5a shows a comparison between the input temperature profile and the reconstructed solutions.

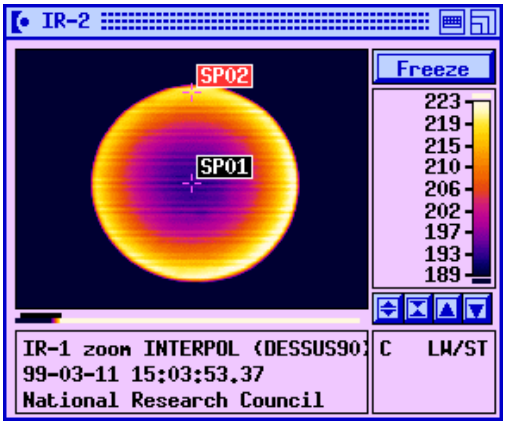

Figure 4. Infrared image of the billet top surface showing the surface-to-core temperature gradient resulting from the "skin effect" during induction heating.

Experimental validation trials were carried out in a three-coil IHS induction heating unit. The material used in the experiments is A356 aluminum alloy. The inverse procedure is validated using the surface temperature recorded by the same infrared camera after the heating was stopped. To make thermal imaging reliable, a high emissivity black paint was used to avoid the problem of emissivity variations with temperature and oxidation during heating. The

effects of power level on the temperature distribution were considered. In these experiments, three power levels were used: a low heating level, a medium heating level and a high heating level. The experimental procedure is as follows. The infrared camera was turned on but was not recording. When the surface temperature read by the infrared camera was around 500°C, the power was turned off and the camera started to record the surface temperature evolution with time. Figure 5b shows the predicted surface-to-core profiles for the three levels. The heat transfer coefficient h was also estimated as described previously by a trial and error method and is given in Table 1.

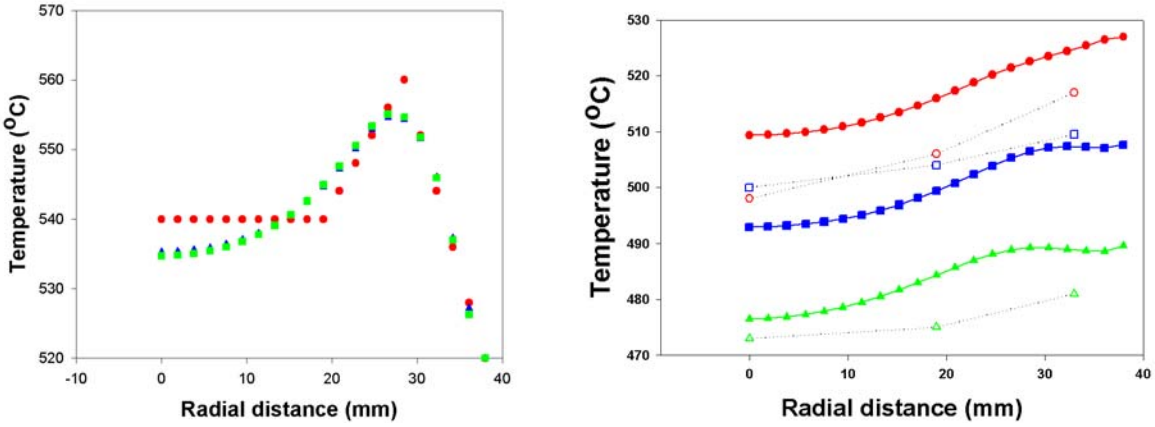

Figure 5. a. Comparison between the input initial temperature profile (() and the reconstructed temperature profiles when the data are exact (%) and when the data contain 2% random noise (▲). **b.** Recovered temperature profiles for the three power levels -High ((), Medium (%) and low (▲)-. Temperature profiles measured with thermocouples for the three power levels -High (O), Medium (э) and low (∈)-.

To validate the temperature inside the billet, three K type thermocouples were inserted from the top of the billet at different radial locations. The results for the three power levels are included in Figure 5b for comparison with those obtained from the inversion.

Discussion: The results reported in Figure 1b, which were obtained from the numerical simulation of the ISBM application, show that when the data are exact, the predicted temperature profile is in excellent agreement with the input except near the sharp corner. This is due to the diffusive nature of the heat equation and/or the smoothing effect of the inverse algorithm. When the data have a 2% random noise, the recovered profile deviates somewhat from the input; however, the error is always less than the noise level even near the sharp corner. This can be considered as very good agreement since it falls within the accuracy of most temperature measurements. As for the temperature profile predicted during the experimental validation of the same application (Figure 3b), it shows a maximum at the center which is due to the high melt temperature. A shoulder is apparent near the outer surface. This could arise from heat generation by viscous dissipation during the filling, but it could also be due to the oscillation from the algorithm. This point is very difficult to evaluate without a direct method to measure the temperature. With regard to the estimated value of the heat transfer coefficient during the real process, it is given in Table 1. The latter value is of the same order of magnitude as those reported in the literature for free convection in air.

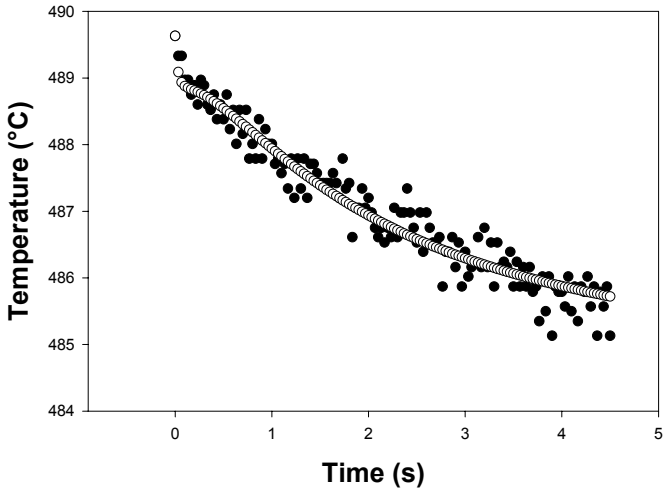

Figure 6. Comparison of the predicted temperature (o) at one point of the surface with the experimental data (() measured with the infrared camera for the low-power experiment.

The simulated results obtained for the SSM forming process and reported in Figure 5a, show that the temperature peak that is visible in the exact profile is represented quite well by the inverse solution. The reconstructed temperature is within 5°C of the input profile with exact or noisy data as shown in Figure 5a. Similar to the ISBM process, the sharp corners have been rounded by the inverse algorithm. The results are somewhat worse since there are two discontinuities in this case and the discontinuity at the peak is more severe than the previous case. However, the fact that the results are very similar with or without noise indicates that the inverse algorithm is quite stable. It should be noted that even though the recovered solution is close to the input profile, the position of the maximum temperature is slightly shifted. As for the predicted profiles obtained from the experimental trials for three different powers (Figure 5b), as expected, the higher is the power, the larger is the deviation between the surface temperature and the core temperature. The deviation between the extreme temperatures was 17°C, 15°C and 13°C, respectively. It is also noted that the shape of the profile changes from one power level to another. This is a result of the mutual competition between the "skin effect", the heat conduction and the heat losses at the surface. For high power level, thermal gradients are nearly constant; the temperature increases almost gradually from the centerline to the surface. In contrast, for medium and low power levels, although the "skin effect" is still dominating, its influence is alleviated by the heat losses at the surface. This is illustrated in the figure by the constant temperature near the surface while the shape of the profiles near the centerline is almost the same for both powers. Furthermore, the comparison with the inserted thermocouples in Figure 5b indicates that the thermocouple readings depict similar shapes retrieved by the inverse technique for each power level. The thermocouple readings also show that at the higher power level, the temperature gradient is steeper in the radial direction, in qualitative agreement with the inversion results. However, there is a serious discrepancy between the identified profiles and the thermocouples, especially for the two higher power levels. It is not evident whether the deviation from the predicted profiles is due to the drawbacks of contact measurement (bad contact between the sensor and the part, local disturbance of the thermal and electromagnetic fields, the drilled billet does not correspond to the model…etc…) or to the inversion algorithm itself. This is still under investigation and yet very difficult to evaluate without a reliable direct method to measure the temperature.

However a very good agreement can be achieved between the predicted surface temperature using, for example, the profile identified for the low power trial and the experimental data related to the same experiment, as presented in Figure 6. This indicates that the minimization algorithm is quite adequate for the problem at hand.

Conclusions: An inverse algorithm was developed to reconstruct the initial temperature profile in a polymer preform and a semi-solid aluminum billet using the surface temperature data. The technique is based on a one-dimensional heat conduction model. A sensitivity study has shown that the unknown parameters can be identified

from two different portions of a given set of surface temperature data. The method was tested using data generated numerically and showed excellent agreement even with addition of 2% random noise. It was then applied to predict the internal temperature of an injection molded preform used in the stretch blow molding process and to an inductively heated aluminum billet at the end of the heating stage in the SSM die-casting process. Reasonable profiles were obtained which need to be verified by other reliable direct methods. Even though it was shown that the inversion procedure could provide a fairly reliable temperature prediction within a few percent, caution should be taken not to overinterpret the results, especially small-scale details.

References: 1. M.C. Flemings, *Behavior of metal alloys in the semi-solid state*, Met. Trans., 1991, A 22, pp.957-981.
2. P. Kapranos, R.C. Gibson, D.H. Kirkwood, and C.M. Sellars, "Induction heating and partial melting of high melting point thixoformable alloys", in *Semi-Solid Processing of Alloys and Composites*, Proceedings of the 4th international conference, Sheffield, 1996, pp.148-152.
3. S. Midson, V. Rudnev, and R. Gallik, "The induction heating of semi-solid aluminum alloys", in *Semi-Solid Processing of Alloys and Composites*, Proceedings of the 5th International Conference, Golden, CO, 1998, pp.497-504.
4. A. Bendada, K.T. Nguyen, and C.A. Loong, "Application of infrared imaging in optimizing the induction heating of semi-solid aluminum alloys", *Advanced Sensors for Metals Processing*, Proceedings of the International Symposium, Quebec city, Canada, 1999, pp.331-342.
5. J.V. Beck, B. Blackwell, and C.R. St. Clair, *Inverse Heat Conduction,* John Wiley & Sons, New York, 1985.
6. A.N. Tikhonov, and V.Y Arsenin, *Solutions of Ill-posed Problems*, Winston, Washington D.C., 1977.
7. D.A. Murio, and D. Hinestroza, *Computers Math Applic.*, **25**, 55-63 (1993).
8. O.M. Alifanov, *Inverse Heat Transfer Problems,* Springer-Verlag, Berlin, 1994.
9. A,J, Silva Neto, and M.N. Ozisik, *Int. J. Heat Mass Transfer*, **37,** 909-915 (1994).
10. R.G. Keanini, and N.N. Desai, *Int. J. Heat Mass Transfer*, **39**, 1039-1049 (1996).
11. D.B. Ingham, and Y. Yuan, *Int. J. Heat Mass Transfer,* **37 Supp.1**, 273-280 (1994).
12. Y. Jarny, M.N. Ozisik, and Bardon, J.P., *Int. J. Heat Mass Transfer*, **34**, 2911-2919 (1991).
13. K.T. Nguyen, and M. Prystay, *Int. J. Heat Mass Transfer*, **42**, 1969-1978 (1999).
14. A. Bendada, and K.T. Nguyen, "Estimation of the initial temperature profile and the heat transfer coefficient in polymer processing by an inverse method", in *Inverse Problems in Engineering: Theory and Practice*, ASME Conference Proceedings, Port Ludlow, WA, 1999, pp.355-361.

K.T. Nguyen, and A. Bendada, *Modelling and Simulation in Materials Science and Engineering*, accepted for publication, (2000).